DOI: 10.1002/((please add manuscript number))
Article type: Communication

Ultrafast Coherent Absorption in Diamond Metamaterials

Artemios Karvounis, Venkatram Nalla, Kevin F. MacDonald, and Nikolay I. Zheludev*

A. Karvounis, Prof. K. F. MacDonald, and Prof. N. I. Zheludev
Optoelectronics Research Centre and Centre for Photonic Metamaterials, University of Southampton, Southampton, SO17 1BJ, UK
E-mail: kfm@orc.soton.ac.uk
Dr. V. Nalla, Prof. N. I. Zheludev
Centre for Disruptive Photonic Technologies & The Photonics Institute, School of Physical and Mathematical Sciences, Nanyang Technological University, Singapore 637371

Keywords: Photonic metamaterials; Diamond; Coherent absorption; Ultrafast

We present the first experimental demonstration of coherent light-by-light modulation at few-optical-cycle (6 fs) pulse durations, enabled by a nanostructured polycrystalline diamond broadband metasurface absorber only 170 nm thick. Photonic metamaterials - artificial media, structurally engineered at the sub-wavelength scale to provide passive and active functionalities not available in natural materials, enjoy considerable attention,[1] not least as planar media with strong, controllable absorption for applications in light energy harvesting, photo-catalysis, photovoltaics, photo-detection and displays. Recently, 'coherent control' of absorption has emerged as a new mechanism for controlling light-with-light,[2,3] with potential applications ranging from signal processing in coherent information networks[4–8] to excitation-selective spectroscopy.[9] The concept is truly scalable, having been demonstrated at wavelengths from visible to microwave,[2,3] and can function at very low intensities (down to the single photon level[10]) and in the quantum regime.[11] It allows for the implementation of various all-optical analogue logical functions in 'four-port devices' (with two inputs and two outputs),[4] which in the simplest case may comprise a thin (substantially sub-wavelength thickness) layer of absorbing material illuminated from both sides by two mutually coherent

light waves representing the two input signals, while the two reflected/transmitted waves constitute the output channels. The coherent redistribution of energy among the four channels and coherently-controlled level of dissipation in the absorber underpin the functionality of such devices: The input beams form a standing wave of electric field within which the thin absorber can be selectively located. At a node it will (in the limit of vanishingly small thickness) experience zero net field and thereby manifest no light-matter interaction (i.e. no absorption) and both beams will propagate as if it were not there; at an anti-node it will be subject to an enhanced field (relative to that of a single incident beam) and absorption will be correspondingly enhanced. A full analytical description of the coherent control paradigm is given elsewhere[2,12] but in summary, for optimal switching contrast the thin film should ideally absorb 50% of traveling wave power across the entire spectrum of the signals involved, and reflect/transmit in equal proportions (i.e. 25% each). Upon this basis it may coherently absorb anywhere between 0 and 100% of incident light depending on the relative phase and intensity of the two inputs at the absorber plane.

Coherent optical gating on thin, resonant plasmonic metamaterial absorbers with continuous wave[12] and 130 fs pulsed[13] beams has previously been demonstrated. The speed of response in coherent signal processing devices is limited only by the width of the absorption line (the former being inversely proportional to the latter), so to exploit the coherent dissipative process for controlling even shorter (few-femtosecond) pulses, a material providing strong, spectrally flat absorption over a very broad wavelength range is required. It should also provide a suitable (ideally 1:1) balance of reflection and transmission, while being capable of withstanding high peak optical intensities. Plasmonic metasurfaces are unable to meet these requirements. However, we report here that a nanostructured, free-standing diamond membrane can exhibit the characteristics necessary for high contrast coherent control of ultrashort (6 fs) optical pulses comprising only a few oscillations of electromagnetic field.

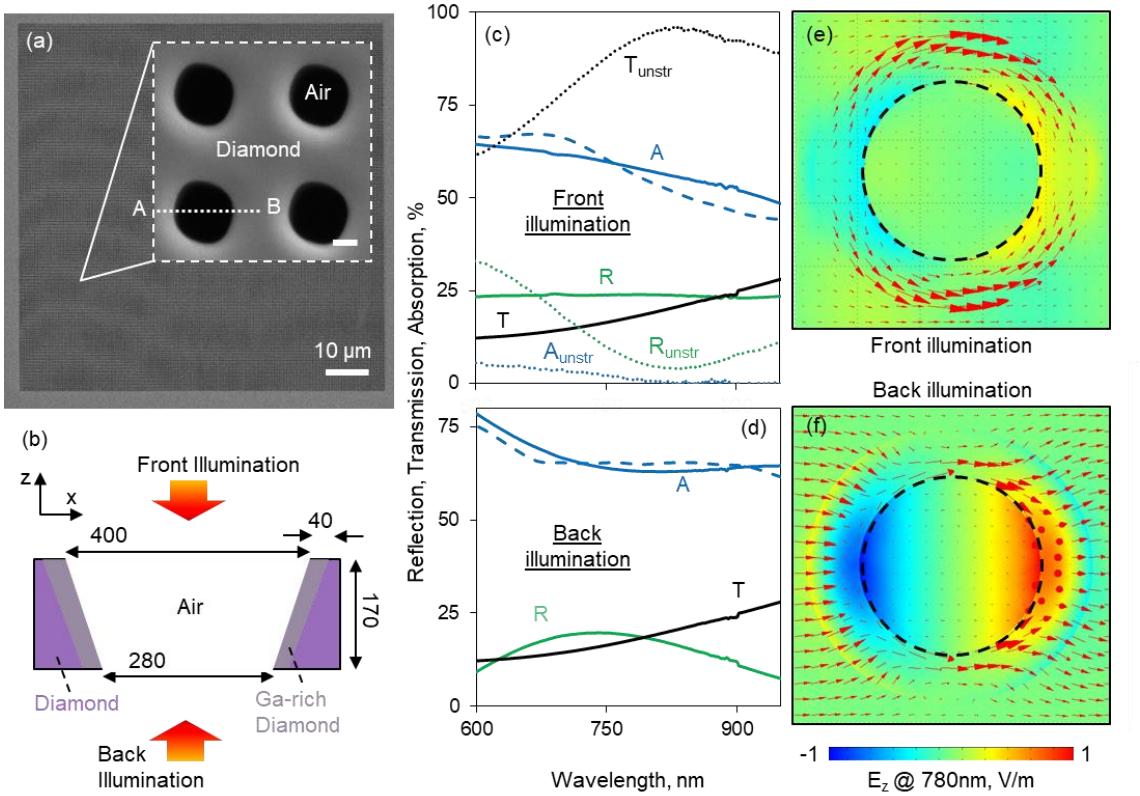

Figure 1. Diamond membrane metamaterial. (a) Scanning electron microscope image of nano-hole array metamaterial, viewed from the front side as defined in panel (b). The inset shows four unit cells of the array at higher magnification [100 nm scale bar]. (b) Schematic cross-section of a metamaterial unit cell [period 500 nm], nominally along line AB in panel (a), with dimensions annotated in nanometres. (c, d) Solid lines - spectral dispersion of normal incidence reflection *R*, transmission *T* and absorption *A* [$=1-\{R+T\}$] for the diamond metamaterial measured using a microspectrophotometer for (c) front and (d) back illumination as defined in panel (b); Dashed lines – numerically simulated metasurface absorption spectra. Dotted lines in panel (c) – measured spectra for the unstructured diamond membrane. (e, f) Numerically simulated field maps showing the distribution of the *z*-component of electric field in the *x*-*y* plane at the midpoint of the membrane in the *z* direction, at a wavelength of 780 nm. Overlaid arrows indicate the direction and magnitude of electric displacement.

Diamond, in the form of single-crystal plates, individual micro/nano-crystals and polycrystalline films, has attracted increasing attention as a photonic material over the past decade:[14,15] for optical waveguide and photonic crystal structures; for its nitrogen-vacancy color centers (which can be harnessed for quantum, sensing and labelling applications); and recently as a platform for mid-infrared 'all-dielectric' metamaterials. Here, we introduce a nanostructured diamond, optical range metamaterial fabricated from a free-standing polycrystalline membrane (**Figure 1**). We show that focused gallium ion beam milling of the

membrane, with a sub-wavelength nano-hole pattern, delivers an elevated level absorption over a VIS-NIR band broad enough to facilitate coherent modulation of few-femtosecond optical pulses.

For the present study, a metamaterial comprising 280 nm diameter nano-holes in a square array of 500 nm period, covering a total area of approximately 100 μm × 100 μm, was fabricated by focused ion beam (FIB) milling in a 170 nm thick polycrystalline diamond membrane (**Figure 1a**; detail of the fabrication process is given in the Experimental Section below). There is inevitably implantation of gallium from the ion source, and this is known to cause stoichiometric changes in a diamond lattice, thereby modifying the mass density, strain and optical properties.[16,17] Indeed, in the present case numerical modelling (presented in Figure 1 and in the Experimental Section) shows that gallium doping, in an estimated 40 nm wide ring around each nano-hole, is largely responsible for the nanostructured membrane's increased VIS-NIR absorption. The structural dimensions employed in computationally simulating the optical properties of the diamond metamaterial are given in the cross-sectional schematic of **Figure 1b** – the off-vertical side walls are a consequence of the FIB milling process, exaggerated here by the necessity of employing a relatively high ion beam current[18] (0.66 nA, giving an angle relative to the vertical of ~20^{o}). Polycrystalline diamond has a refractive index (evaluated by variable angle spectroscopic ellipsometry) n_D = 2.4 across the 600-950 nm spectral range of interest, while gallium-doped diamond is taken to have a refractive index n^* = 3.45 + 0.6i (see Experimental Section). With a unit cell size of 500 nm the metasurface is non-diffracting throughout the experimental wavelength range; It has four-fold rotational symmetry and so its properties do not depend on the polarization state of incident light; But they are directionally asymmetric in consequence of the tapered hole profile, as illustrated by the spectra in **Figures 1c and 1d**. **Figures 1e and 1f** present the distributions of normalized out-of-plane electric field and in-plane displacement currents for the two directions of illumination ('front' and 'back' as denoted in Figure 1b) at 780 nm - the

central wavelength of the fs-pulsed laser source employed in experiments (below). At this wavelength, transmission *T* is 18% (in both propagation directions, as must be the case in a linear reciprocal medium), reflection *R* is 18% for front illumination versus 24% from the back, and absorption levels (evaluated as 1-{ *R* + *T*}) correspondingly differ by 6% for the two directions. Back illumination excites an electric dipole parallel to the incident polarization direction in the plane of the membrane, leading to a characteristic broad reflection resonance, with a peak in this case at a wavelength of 740nm (Figure 1d). In contrast, no resonant features are apparent for front illumination and the reflection spectrum is almost flat (Figure 1c). For both directions of propagation the proportionality among transmission, reflection and absorption is less than ideal for a 'coherent absorber', but the diamond metasurface does meet the most fundamental requirement of maintaining an elevated and weakly-dispersive level of absorption over a spectral range greater than the ~100 nm bandwidth of ultra-short (few-fs) laser pulses (and greater than the typical linewidth of plasmonic metasurface resonances[4,9,10,12,13]).

The experimental short-pulse coherent modulator configuration is illustrated schematically in **Figure 2**. A train of femtosecond laser pulses (with a durations adjustable down to ~6 fs and a center wavelength tunable from 650 to 975 nm, is divided by a pellicle into two (collinearly polarized) 'input' beams focused at normal incidence from opposite sides onto the diamond metamaterial by a pair of focusing mirrors. The metamaterial is mounted on a piezoelectric translation to facilitate the setting/tuning of the relative time delay, and thus the relative phase difference, between corresponding pulses from the two input channels. The two output beams (transmitted and reflected from both sides of the metamaterial) are directed via pellicle beam splitters to a pair of identical photodiodes.

In keeping with the behavior reported in Ref. [13] for a plasmonic metasurface probed using much longer 130 fs pulses, the output signal here is seen to oscillate between coherently-suppressed and -enhanced levels as a function of the time/phase delay between the incident 6

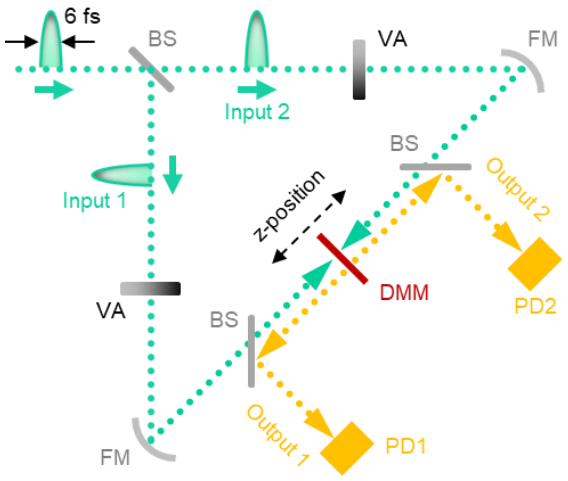

Figure 2. Experimental arrangement for measurement of short-pulse coherent absorption modulation in a diamond membrane metamaterial. The input beam is provided by a 6 fs Ti:sapphire oscillator via a pulse shaping system, which is employed to tune the duration and center wavelength of pulses. (BS = pellicle beam-splitter; VA = variable attenuator; FM = focusing mirror; DMM = diamond metamaterial; PD = photodiode).

fs pulses in the diamond metamaterial plane, within an envelope defined by their temporal overlap (**Figure 3a**). The signal is high (coherent absorption low) when the metamaterial is located at the nodes of the electric field standing wave formed by the input beams, and vice-versa at the anti-nodes. The zero-delay position is taken to be the point at which magnitude of coherent absorption is maximized (i.e. output signal minimized); the oscillation period corresponds to a distance of half of the center wavelength of the incident pulses. At large positive and negative delays, when there is no overlap between incident pulses in channels 1 and 2, the output signal is constant at a level corresponding to the total incoherent absorption of the two input beams by the metamaterial. The discrepancy in the amplitude of coherent modulation between the two output channels is a consequence of the directional asymmetry of the metamaterial discussed above.

We define the coherent modulation depth as: $\frac{P_{max}-P_{min}}{P_{max}+P_{min}}$, where P_{max} and P_{min} are respectively the highest and lowest output signal levels (averaged over the two output channels) achieved around the zero-delay point (as annotated in Figure 3a). A modulation depth of between 0.34 and 0.41 is maintained by the diamond metasurface for pulse durations ranging all the way

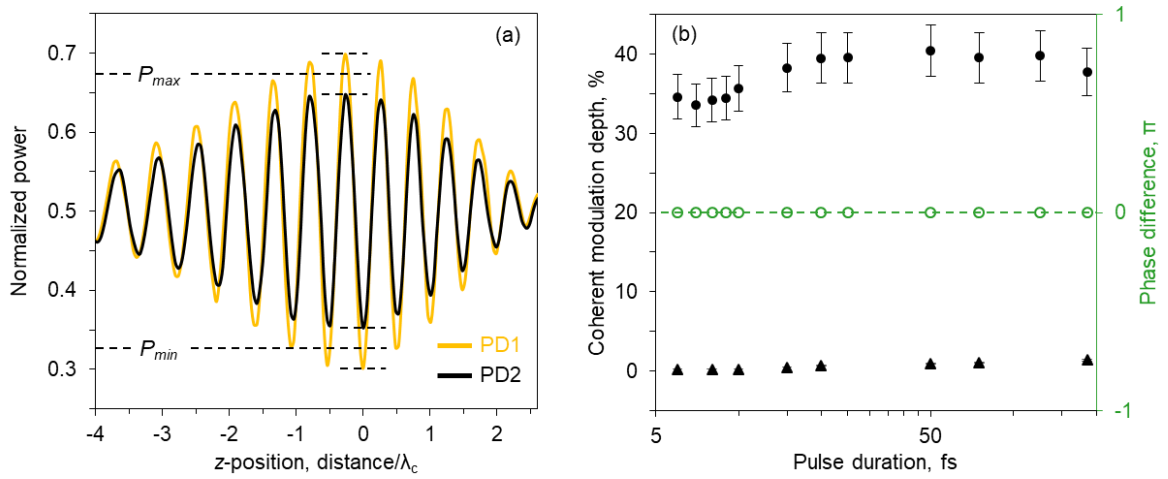

Figure 3. Ultrashort pulse modulation using a diamond metamaterial. (a) Dependence of output power in channels 1 and 2 [orange and black lines respectively, relative to input power per channel] on the z-position [as defined in Figure 2] of the metamaterial, i.e. on the temporal delay between counter-propagating incident 6 fs pulses at a center wavelength λ_c = 780 nm. (b) Coherent modulation depth as a function of pulse duration for the diamond metamaterial [filled circles] and for the unstructured diamond membrane [triangles], and for the former the phase difference between output channels 1 and 2 [open circles].

from 185 fs down to 6 fs (**Figure 3b**), in contrast to the unstructured diamond membrane which is to all intents and purposes is non-absorbing. There is zero phase difference between the two output channels across the entire range of pulse durations. This behavior is markedly different from that observed with plasmonic metamaterial coherent absorbers, where the output channels shift increasingly out of phase as the pulse duration falls below ten femtoseconds (such that the metasurface starts to behave like a mirror),[19,20] thereby limiting the modulation bandwidth. The diamond metasurface retains its absorptive nature at ultra-short pulse durations (down to at least 6 fs) because its absorption band is characteristically much wider than the plasmonic absorption peak in a gold nanostructure.

Moreover, the coherent modulation depth achieved with the diamond metamaterial remains approximately constant, with again zero phase difference between the two output channels, while the short-pulse center wavelength is tuned all the way from 650 to 975 nm (the entire tuning range of the laser source), as shown in **Figure 4** for pulse durations of 50 fs (19 nm

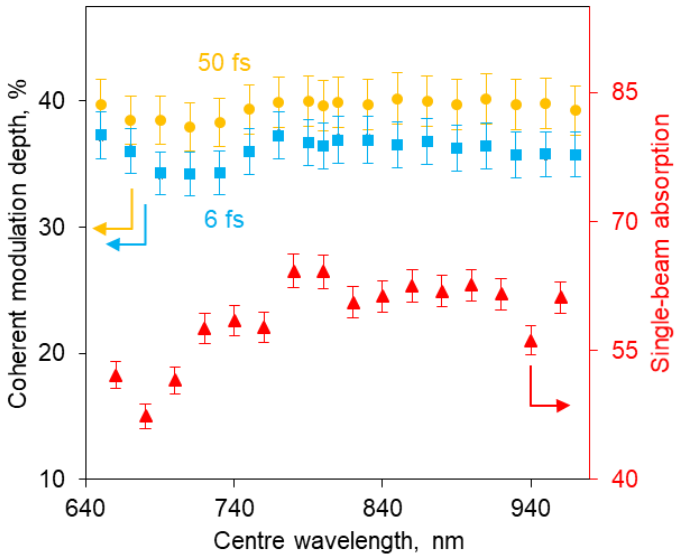

Figure 4. Ultrashort pulse modulation using a diamond metamaterial – spectral dispersion. Dependence of coherent modulation depth on center wavelength for pulse durations of 6 fs [square symbols] and 50 fs, at a fixed fluence of 0.4 nJ/cm^2, overlaid with the single-beam absorption spectrum for 50 fs pulses illuminated from the front, evaluated as $1-\{R+T\}$ when blocking one of the two pulsed input beams [whereby one of the output channels records reflection and the other transmission].

bandwidth) and 6 fs (157 nm bandwidth). The only perturbation over this spectral range is a small dip in the magnitude of coherent absorption modulation at around 700 nm, corresponding to a dip in the single-beam absorption spectrum overlaid in **Figure 4**. Once more, this performance stands in marked contrast to that of plasmonic metasurfaces, for which the amplitude of coherent absorption modulation is strongly dispersive by virtue of their relatively narrow absorption resonances.[4,9,10,12,13]

In conclusion, we have experimentally demonstrated a free-standing diamond membrane metamaterial as a broadband, polarization-independent absorber for the visible to near-infrared wavelength range, serving as the functional element of a coherent optical modulator providing modulation contrast up to 4 dB with a bandwidth of 160 THz. The underlying control mechanism is a strictly linear interference effect and as such may be implemented at arbitrarily low intensities, and does not induce harmonic distortion of signals. Ultrafast coherent modulation functionality is demonstrated here over the 650–975 nm wavelength

range of the experimental short-pulse laser platform, but the device concept can be implemented across a broader VIS-NIR range with appropriate variation of the metamaterial design and/or dimensions. Modulation contrast may be enhanced with design optimization to achieve identical levels of absorption (nearer 50%) for both directions of light propagation through the metamaterial and better matched levels of reflection and transmission. That said, 4 dB contrast is a level already considered adequate for some optical interconnect applications.[21] The upper limit on coherent modulation bandwidth for the diamond metasurface is considerably higher than the ~100 THz level observed for plasmonic metasurfaces, and indeed lies beyond the measurable range in the present study (where the shortest available pulse duration is ~6 fs). As a material platform for photonic metamaterials, diamond membranes may also present a number of advantages (over plasmonic counterparts) in terms of physical/chemical robustness, optical power handling, and amenability to doping, thereby enabling a variety of otherwise impractical ultra-short pulse, nano-opto-mechanical and quantum device functionalities.

Experimental Section

Diamond membranes: Our experiments employ polycrystalline diamond membranes (on silicon frames, with a clear aperture of 300 μm diameter) by Applied Diamond Inc.

Focused ion beam milling: Metamaterial arrays of nano-holes are milled through the diamond membrane using an FEI Helios NanoLab 600 focused ion beam (FIB) system. Each hole was formed by holding the ion beam, with an acceleration voltage of ~30 keV and beam current of 0.66 nA, at a fixed point for 600 ms (delivering of order 1×10^{18} ions/cm^2; and an etch rate of ~0.02 μm^3/nC).

Variable-angle spectroscopic ellipsometry: The complex relative permittivity / refractive index of CVD diamond was evaluated by spectroscopic ellipsometry (J. A. Woollam 4000) over the wavelength range from 400 – 1600 nm.

Microspectrophotometry: Reflection and transmission spectra were obtained using a microspectrophotometer (CRAIC QDI2010), with a 30 μm × 30 μm sampling aperture. Measurements were taken via a 36× objective and 0.52 NA and therefore represent an average over incident angles ±28^{o} about the surface normal. All data are normalized to reference levels for air (100% transmission), a silver mirror (high reflector) and a 'Vantablack' vertically-aligned carbon nanotube array (zero reflection/transmission).

Short-pulse coherent absorption measurements: A pulse shaping system (MIIPSBOX640 by Biophotoinc Solutions Inc.) was used to tune the center wavelength (from 650 to 970 nm) and spectral width (from 5 to 165 nm, corresponding to pulse durations from 185 to 6 fs) of pulses from a Ti:sapphire oscillator (Femtolasers Rainbow). The laser beam was subsequently divided using a 50:50 pellicle beam-splitter and a pair of broadband enhanced-Ag focusing mirrors (150 mm radius of curvature) was used to focus the two beams at normal incidence from opposing sides to a spot diameter of ~50μm on the diamond membrane, which was mounted on a piezoelectric translation stage moving parallel to the incident beam direction. The average power of the two input beams at the sample position was balanced for each setting of pulse duration and center wavelength using a variable neutral density filter and maintained at a level of ~1μW per beam (sufficiently low as to exclude nonlinear effects). The pulse shaper was configured to optimize the pulse profile at the sample position rather than at its own output port (i.e. to compensate for the dispersion of intermediate optical components). The two output beams (comprising transmitted and reflected beams from both sides of the sample) were directed via two more pellicle beam-splitters (25:75) to a pair of identical photodiodes, the outputs from which were monitored using lock-in amplifiers referenced to the 130 Hz frequency of a mechanical chopper located at the output of the pulse shaper. Signal levels were calibrated for each measurement using an aperture in the diamond membrane, so as to eliminate effects such as due to the spectral dispersion of the pellicles' power splitting ratio.

Numerical Simulations: Full-wave electromagnetic simulations of the metamaterial structure, based on the geometry presented in Figure 1b, were performed using the finite element method in COMSOL Multiphysics. Calculations employ periodic boundary conditions in the *x* and *y* directions and assume normally incident, narrow-band, coherent illumination. Unstructured polycrystalline diamond is taken to have a non-dispersive refractive index n_D = 2.4 across the entire spectral range of interest (evaluated by spectroscopic ellipsometry); Parameters for gallium-rich diamond are estimated from a fitting of numerically simulated spectra to the metasurface's measured absorption spectra (Figure 1). We assume that there is a uniformly doped 'collar' of diamond formed around each nano-hole, with a thickness of 40 nm (an ion penetration range consistent with prior studies of diamond,[16,17] and with a 'Stopping Range of Ions in Matter' [SRIM][22] Monte Carlo method model). Ion implantation is known to increase both the real and imaginary parts of refractive index: **Figure 5** presents the evolution of diamond metasurface spectra with the refractive index n^* of the Ga-doped collar, alongside simulated spectra for the unstructured diamond membrane. The latter, inevitably given that it has an imaginary part of refractive index equal to zero, shows zero absorption. (The few percent of absorption seen at shorter wavelengths in the experimental absorption spectrum for unstructured polycrystalline diamond (Fig. 1c) is attributed to scattering, which is indistinguishable from absorption evaluated as $1-\{R+T\}$.) In the absence of doping (i.e. in the absence of any index change, when $n^* = nD$), nanostructuring introduces high-quality reflection and transmission resonances but no absorption. These resonances are heavily damped and spectrally shifted as the real and imaginary parts of refractive index increase (with increasing Ga doping), eventually merging to form a broad absorption band. An doped-diamond refractive index value of 3.45-0.6i is found to produce a good correlation with experimentally measured spectra; for comparative reference Fig. 5 also presents spectra for higher and lower index values.

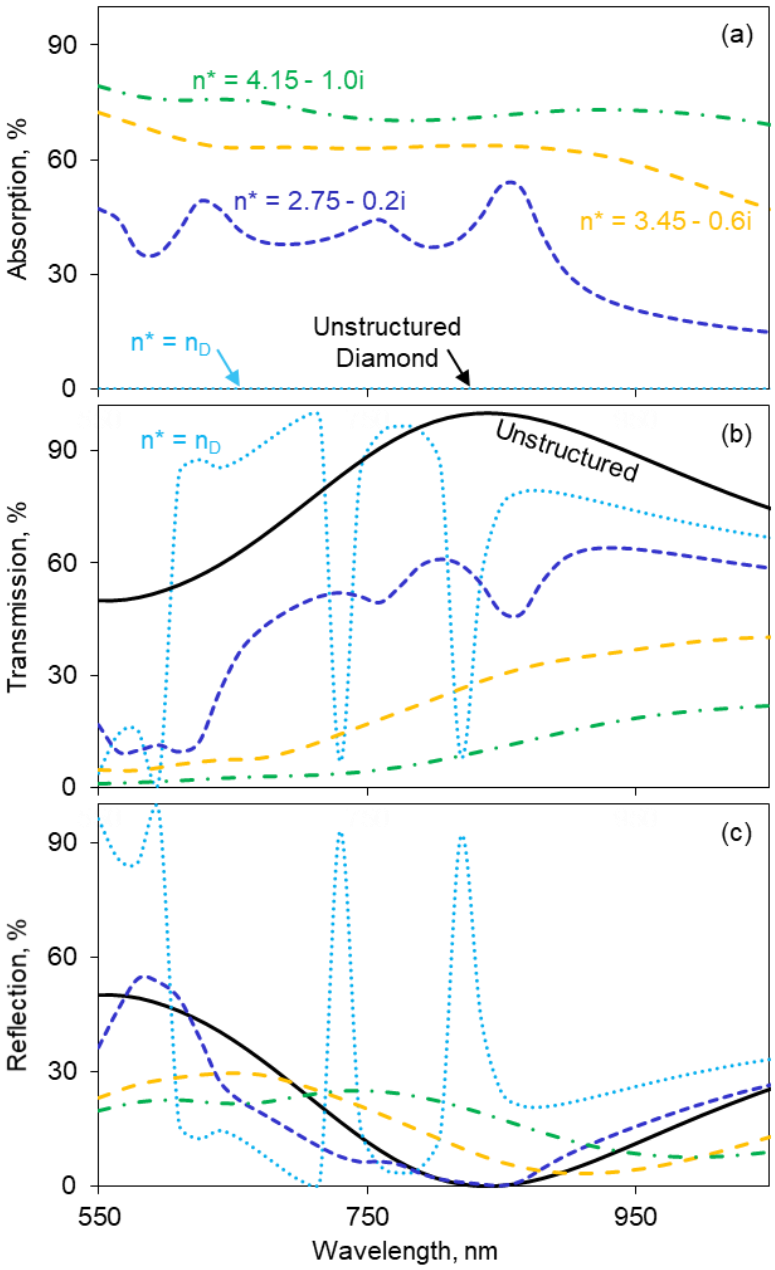

Figure 5. Dependence of metasurface optical properties on refractive index change in gallium-doped diamond. Numerically simulated absorption, transmission and reflection spectra for diamond membrane nano-hole metasurfaces of the geometry presented in Fig. 1b [back illumination], for varying values of refractive index n* [as labelled] in the doped collar around each hole. Simulated spectra for the unstructured diamond membrane [refractive index n_D = 2.4] are also shown.

Supporting Information

Following a period of embargo, the data from this paper can be obtained from the University of Southampton ePrints research repository: http://doi.org/10.5258/SOTON/D0197

Acknowledgements

A.K. and V.N contributed equally to this work, which is supported by the UK Engineering and Physical Sciences Research Council [grant EP/M009122/1] and the Ministry of Education, Singapore [grant MOE2011-T3-1-005].

Received: ((will be filled in by the editorial staff))

Revised: ((will be filled in by the editorial staff))

Published online: ((will be filled in by the editorial staff))

References

[1] A. M. Urbas, Z. Jacob, L. D. Negro, N. Engheta, A. D. Boardman, P. Egan, A. B. Khanikaev, V. Menon, M. Ferrera, N. Kinsey, C. DeVault, J. Kim, V. Shalaev, A. Boltasseva, J. Valentine, C. Pfeiffer, A. Grbic, E. Narimanov, L. Zhu, S. Fan, A. Alù, E. Poutrina, N. M. Litchinitser, M. A. Noginov, K. F. MacDonald, E. Plum, X. Liu, P. F. Nealey, C. R. Kagan, C. B. Murray, D. A. Pawlak, I. I. Smolyaninov, V. N. Smolyaninova, D. Chanda, *J. Opt.* **2016**, *18*, 93005.

[2] E. Plum, K. F. MacDonald, X. Fang, D. Faccio, N. I. Zheludev, *ACS Photonics* **2017**, acsphotonics.7b00921.

[3] D. G. Baranov, A. Krasnok, T. Shegai, A. Alù, Y. Chong, *Nat. Rev. Mater.* **2017**, *2*, 17064.

[4] X. Fang, K. F. MacDonald, N. I. Zheludev, *Light Sci. Appl.* **2015**, *4*, e292.

[5] J. M. Rothenberg, C. P. Chen, J. J. Ackert, J. I. Dadap, A. P. Knights, K. Bergman, R. M. Osgood, R. R. Grote, *Opt Lett* **2016**, *41*, 2537.

[6] Z. J. Wong, Y.-L. Xu, J. Kim, K. O'Brien, Y. Wang, L. Feng, X. Zhang, *Nat. Photonics* **2016**, *10*, 796.

[7] R. Bruck, O. L. Muskens, *Opt. Express* **2013**, *21*, 27662.

[8] A. K. Jahromi, A. F. Abouraddy, *arXiv:1706.04968v1* **2017**, *40*, 5550.

[9] X. Fang, M. L. Tseng, D. P. Tsai, N. I. Zheludev, *Phys. Rev. Appl.* **2016**, *5*, 1.

[10] T. Roger, S. Vezzoli, E. Bolduc, J. Valente, J. J. F. Heitz, J. Jeffers, C. Soci, J. Leach, C. Couteau, N. I. Zheludev, D. Faccio, *Nat. Commun.* **2015**, *6*, 7031.

[11] Q. P. Su, H. H. Zhu, L. Yu, Y. Zhang, S. J. Xiong, J. M. Liu, C. P. Yang, *Phys. Rev. A* **2017**, *95*, 1.

[12] J. Zhang, K. F. MacDonald, N. I. Zheludev, *Light Sci. Appl.* **2012**, *1*, e18.

[13] X. Fang, M. L. Tseng, J.-Y. Ou, K. F. Macdonald, D. P. Tsai, N. I. Zheludev, *Appl. Phys. Lett.* **2014**, *104*, 141102.

[14] I. Aharonovich, A. D. Greentree, S. Prawer, *Nat. Photonics* **2011**, *5*, 397.

[15] M. J. Burek, N. P. De Leon, B. J. Shields, B. J. M. Hausmann, Y. Chu, Q. Quan, A. S. Zibrov, H. Park, M. D. Lukin, M. Loncar, *Nano Lett.* **2012**, *12*, 6084.

[16] M. A. Draganski, E. Finkman, B. C. Gibson, B. A. Fairchild, K. Ganesan, N. Nabatova-Gabain, S. Tomljenovic-Hanic, A. D. Greentree, S. Prawer, *Diam. Relat. Mater.* **2013**, *35*, 47.

[17] S. Rubanov, A. Suvorova, *Diam. Relat. Mater.* **2011**, *20*, 1160.

[18] W. C. L. Hopman, F. Ay, W. Hu, V. J. Gadgil, L. Kuipers, M. Pollnau, R. M. De Ridder, *Nanotechnology* **2007**, *18*, 195305.

[19] V. Nalla, S. Vezzoli, V. João, S. Handong, N. Zheludev, in *Eur. Conf. Lasers Electro-Optics - Eur. Quantum Electron. Conf.*, **2015**.

[20] V. Nalla, J. Valente, H. Sun, N. I. Zheludev, *Opt. Express* **2017**, *25*, 22620.

[21] F. Y. and T. D. J. Reed G T, Mashanovich G, Gardes, *Nat. Photonics* **2010**, *4*, 518.

[22] J. F. F.Zeigler, J. P. Biersak, “SRIM2008,”